Tabašević, I. D., *et al.*: Experimental and Numerical Investigation of Thermal and ...
THERMAL SCIENCE: Year 2022, Vol. 26, No. 1B, pp. 801-814

801

EXPERIMENTAL AND NUMERICAL INVESTIGATION OF THERMAL AND FLOW CONDITIONS INSIDE A LARGE PHARMACEUTICAL STORAGE AFTER THE VENTILATION SYSTEM FAILURE

by

Ilija D. TABAŠEVIĆ[a*], Rastko D. JOVANOVIĆ[b], and Dragan D. MILANOVIĆ[c]

[a] Equipment and System Qualification and Calibration Department,
Hemofarm, Vrsac, Serbia
[b] Department of Thermal Engineering and Energy,
Vinca Institute of Nuclear Sciences,
National Institute of the Republic of Serbia,
University of Belgrade, Belgrade, Serbia
[c] Faculty of Mechanical Engineering, University of Belgrade, Belgrade, Serbia

Safe storage of pharmaceutical products is of great importance due to potential hazards for human health. The aim of this study was to assess the ability of pharmaceutical storage to recover design temperature during ventilation system recovery. The performed CFD simulations showed good agreement with experimental temperature measurements. Numerical results allowed in-depth analysis of flow field and temperature distribution inside the storage. It was discovered that the flow field is highly non-uniform, which consequently leads to an uneven temperature distribution of pallets with products. However, a high inlet mass-flow rate ensured that all pallets reach the designed temperature.

Key words: *pharmaceutical storage, pallets, thermal conditions, flow field, CFD, air distribution systems, system failure*

Introduction

Maintaining stable and controlled design temperature inside pharmaceutical storage has great importance on preventing possible losses in products' quality and safety. With the advancement of air refrigeration and ventilation systems this area of research gained a significant interest within scientific and professional communities [1, 2] the handling of environmental conditions experienced by products along the supply chain assumes increasing relevance. The storage temperature is one of the most important drivers in controlling the physicochemical properties of a perishable product throughout the distribution chain. Therefore, a fair strategy for ensuring the quality and safety of products to the final consumer is to monitor the temperature conditions experienced by products during their storage time spent in warehouses, through dedicated location-mapping activities. However, the warehousing literature reveals a lack of methods and tools to lead managers through temperature warehouse mapping. In view of this, this chapter proposes a tool tailored for the calculation and visualization of temperature profiles of each storage location over a given time period. The proposed tool is validated through a multiple case study provided by two third-party logistics

---

* Corresponding author, e-mail: ilija.tabasevic@hotmail.com

Ho *et al*. [3] presented the results of numerical simulations of temperature and velocity fields inside a cooled warehouse. The studied refrigerated warehouse had a series of cooling units built in ceiling in front stacks with product packages. Both 3-D and 2-D models were calculated. The obtained results from both models were congruent. A parametric analysis was performed in the next step using the equivalent model with varying air velocity and positions of the cooling units. It was found that a better cooling effectiveness and more uniform temperature can be achieved by using higher air velocity and/or positioning the cooling units lower and closer toward the product packages.

Wu *et al*. [4] performed a CFD study of heat transfer and velocity distribution inside a high-bay depot. The main aim of their work was to find the most appropriate air supply and energy-saving method. For example, the results of a supply-air method of high-bay depot study pointed out that the diameter and spacing of the supply-air inlets greatly influence temperature distribution. The temperature non-uniformity coefficient during summer is lower than the one in winter. The obtained results are useful as a theoretical background for the high-bay depot design and economical operation.

Hoang *et al*. [5] performed a transient CFD simulation of the cooling process inside a room with four apple pallets. Two different CFD models of transient heat transfer by forced convection in a cold room filled with apple pallets were investigated and compared against experimental data. In the first approach, each apple pallet was modeled as a single porous medium block. In the second, each pallet was modeled as eight solid blocks, each representing a single apple bin. Both approaches showed a good agreement with the experimental results in terms of air velocity and product temperature change during cooling process. A somewhat more accurate prediction of product temperature change was obtained with the solid block approach. The porous medium approach also produced a satisfying result with a much coarser mesh (nearly four times). Four turbulence models (standard k-ε, RNG k-ε, realizable k-ε, and shear stress transport (SST) k-ω) and two heat transfer models for porous medium (local thermal equilibrium and local thermal non-equilibrium model) were tested. The SST k-ω was found to be the most appropriate for the investigated configuration.

Kaood *et al*. [6] performed a CFD based investigation of the flow field and temperature distribution inside a large cold store for frozen food. The authors used CFD technique to adequately predict the cold storage air-flow distribution inside the cold room cooled with various evaporator's arrangements of sizes, numbers and positions. The main parameters were local temperatures and velocity distributions inside a large cold store. Turbulence was modeled using standard k-ε model on computational mesh consisting of 5400000 tetrahedral elements. Different optional designs with different evaporators' numbers and locations were utilized for load estimation of the cold store. Authors concluded that using a large number of evaporators gives more uniform flow field and minimizes presence of dead zones. Similarly, it is not favorable to use two evaporators for the large cold store because it will lead to a generation of large dead zones with a high temperature and low velocity.

Parpas *et al*. [7] performed experimental measurements and CFD analysis of temperature and flow characteristics inside a laboratory-scale test facility. Chilled food manufacturing facilities are usually cooled by fan coil units located at ceiling level similarly to cold rooms, resulting in high velocity magnitudes, uncomfortable working environments, and high energy consumption. To address these issues, authors investigated the influence of different air distribution arrangements on air. The main aim of the performed simulations was to obtain low velocities and uniform temperatures at human level and to achieve temperature stratification between floor and ceiling levels to reduce energy consumption. Experimental and CFD modelling results showed that supplying air at medium level in the space through special fabric ducts

socks could provide temperature stratification of the order of 7 °C between floor and ceiling level and achieve energy savings in the region of 9% compared to ceiling mounted fabric ducts and 23% over non-ducted cooling coils mounted at ceiling level.

Sularno *et al*. [8] studied temperature flow field characteristics inside a cold room filled with pharmaceutical bottles. Temperature distribution and the storage cooling performance were studied using experimental measurement and numerical simulation. It was shown that variation of bottle arrangement and rack arrangement impacts temperature distribution and cooling performance of cold storage. Surface temperatures of the bottles were measured for all investigated bottles and rack arrangements. The initial temperature of cold storage was set to 5 °C. A transient 3-D CFD model was suggested and used to assess the cooling performance and temperature distribution inside a bottle. Numerical simulation showed that rack arrangement, parallel with the cold room fan, and *V*-shaped bottle lay-out provides a good cooling performance. Using this arrangement, it takes 1480 minutes to reach a stable temperature at the setpoint, and an optimum temperature distribution (with temperature difference of 0.58 °C).

Parpas *et al*. [9] performed experimental measurements and numerical modelling of real food cold room. The paper investigates thermal environment in existing food manufacturing facilities, with two different air distribution systems: supply/return diffusers and fabric ducts. The study was performed by means of both in-situ measurements and 3-D CFD simulations. Both experimental measurements and CFD simulations showed that the fabric duct provides a better environment inside the processing area providing more uniform flow patterns compared to those with the diffusers. Temperature stratification was used as the key indicator for improvement of energy use inside cooling space. Additional numerical simulations confirmed that air temperature stratification improves by moving the fabric ducts from ceiling to a medium level. This resulted in a temperature gradient increase up to 4.1 °C in the unoccupied zone.

Ghiloufi and Khir [10] used 3-D CFD simulations to suggest a novel food cold store design based on air deflector profiles. The main aim of this study was to define the most favorable precooling conditions, which would produce uniform temperature distribution inside the room. The considered cold room had a volume of 67 m^3 and operated with an evaporator giving the providing required refrigeration capacity. The 3-D CFD model was developed taking into consideration the local environmental parameters. Turbulence SST *k-ω* model was used to calculate the air turbulences. For the standard design of the cold store room and during the precooling period of 40 hours, the air velocity and temperature were measured in the different locations inside the room. The measured values varied between 0.25-7 m/s and 3-6 °C. At the same time, the product temperature was higher than the required for about 12 °C. A new cold store room design was suggested, based on special aerodynamic air deflector profiles. This allowed for improvements of the heat transfer between the cold air and product. The use of the new design reduced the precooling period for 10 hours and the average product temperature decreased to 6 °C.

Tanaka *et al*. [11] performed an unsteady 3-D CFD simulation assess the cooling performance of a cold store in cooling process. Turbulence was modeled using standard *k-ε* model with standard wall functions. The model was successfully validated by comparison with cooling experiments. Different loading patterns of corrugated fiberboard containers filled with products in a cold store were simulated. As a result, flat loading with air gaps was the optimal configuration achieve uniform temperature and rapid cooling.

Špiljar *et al*. [12] modeled the jet fan ventilation system in an underground car park. The performed work described a numerical model used to analyze air stagnation areas, air-flow and streamline patterns and the influence of partition walls on the jet fan ventilation system. Additionally, focus was put on the validity of the choice of the jet fan ventilation system for the

underground car parks with partition walls. The obtained results showed that jet fan ventilation system is not suitable for all underground car park architecture lay-outs.

Guo *et al*. [13] used CFD simulations to determine the characteristics of humidity control in a fresh-keeping container. A pressure gauge was used to measure the ventilation resistance of products, by which the inertial resistance and viscous resistance values were obtained. The results of humidity performance were evaluated according to the entropy method. The results showed that the number of ultrasonic atomizers and the sensor location had a significant effect on the humidifying rate. The results of the study provide a better understanding of humidity control, which will in turn help the environment control in a fresh-keeping container.

Sajadiye and Zolfaghari [14] performed CFD based study to determine if the cooling performance of fruit and vegetables inside the cool storages was affected by pallet boxes arrangement. The effect of two different types of vented pallet boxes arrangements, including in-line and staggered on cooling performance were compared using CFD models of air-flow and heat and mass transfer. Results showed that staggered array increased the surface heat transfer coefficient at the pallet boxes wall, which caused reduction in cooling time compared to the in-line configuration. However, staggered array did not improve temperature homogeneity and moisture loss.

Storages are commonly built in accordance with prescribed standards and based on previous experiences. Although this approach ensures that desired conditions inside the storage are maintained, it may also lead to an increased energy consumption and non-uniform temperature and velocity fields. Although a number of scientific papers dealing with CFD simulation of temperature and flow conditions inside cold rooms were published in the last several years, the vast majority of these focus on food storage conditions and only a few deal with the storage of pharmaceutical products [2].

The main aim of this work is to bridge the existing gap by proposing a hybrid CFD model for the simulation of thermal patterns and velocity flow fields inside a real pharmaceutical storage. The main novelty of this model is its ability to simulate both steady-state and transient 3-D turbulent flows in the computational domain with complex geometry and large dimensions. To the best of the authors' knowledge, such studies are not reported in the relevant scientific literature. The suggested model of the pharmaceutical storage was used to investigate the storage capacity to achieve design working parameters after a ventilation system failure.

Experimental investigation

Taking into account the standards and guidelines established by the relevant regulatory acts [15-17] a temperature mapping experiment was performed in a pharmaceutical warehouse. Wireless Rotronic HC2A-S3 data loggers were used in the experiment, with a factory calibration certificate (measurement accuracy ±0.1 K at 296.15 K, repeatability 0.05 K). Data loggers' T63 response was <15 seconds. The time between two consecutive measurements was 1 minute. The temperature in the warehouse was regulated by the HVAC system, which was initially set at 294.65 K. The experiment was performed in three phases. For the purposes of the first phase of the experiment, from December 31st, 2020, at 12.32 p. m. the warehouse temperature was gradually lowered to 291.15 K, after which the system was restored to the initial value of 294.65 K on January 2nd, 2021 at 1.22 p. m. The second phase of the experiment was the system recovery period. This phase lasted from 1.22 p. m. to 6.00 p. m. on January 2nd, 2021, during which the temperature was lowered to the allowed minimum of 293.15 K. The third phase of the experiment was the complete system recovery period. This phase lasted from 1.22 p. m. on January 2nd, 2021 to 13.00 p. m. on January 4th, 2021, during which the temperature was recovered to the initial value of 294.65 K. The goal of the experiment was to measure

Tabašević, I. D., *et al.*: Experimental and Numerical Investigation of Thermal and ...
THERMAL SCIENCE: Year 2022, Vol. 26, No. 1B, pp. 801-814

805

the air temperature at the 27 specified positions within the warehouse and to compare the experimental and numerical data. Data loggers were positioned according to the fig. 1(a). Three data loggers were placed at a particular height at each shown position. Data loggers, fig. 1(c), are labelled in the format X, Y, Z. The X indicates the rack number, and can be marked with 4, 15, or 25, fig. 1(b). The Y indicates the pallet place number, and can be marked with A, B, or C. The Z indicates the height of the data logger's position according to the tab. 1.

Figure 1. Data loggers positions (a), pallet racks (b), and detail view of data logger (c) (in rectangle)

Table 1. Positions of data loggers

	Rack 4	Rack 15	Rack 25
Height 1	1500 mm	1500 mm	1500 mm
Height 2	6200 mm	6600 mm	6650 mm
Height 3	10450 mm	11000 mm	11600 mm

Mathematical model

Geometry model

The real storage front view is shown in fig. 2. The modeled storage geometric domain was simplified, omitting storage space below the storage roof. This was done in order to simplify computational mesh generation and increase CFD calculation stability. It is important to point out that the accuracy of the solution was not affected by this simplification since the air in the near-roof zone is stagnant and does not have a significant role in the pallets' heating process. Moreover, air inlets and outlets were positioned below the near-roof surface, further justifying the adopted simplification.
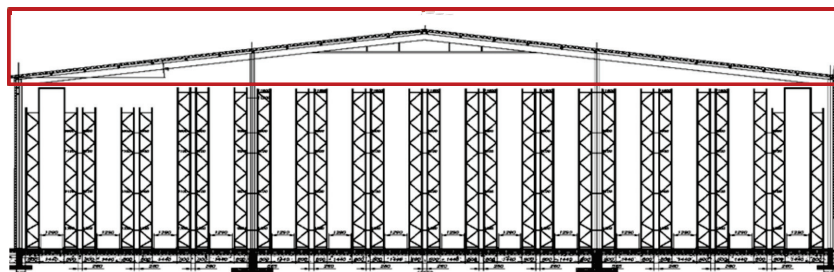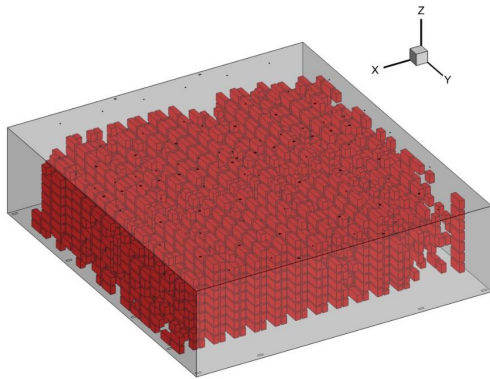

Figure 2. Pharmaceutical storage with pallets, front view − storage space inside the red square is omitted from the model

Tabašević, I. D., *et al.*: Experimental and Numerical Investigation of Thermal and ...
THERMAL SCIENCE: Year 2022, Vol. 26, No. 1B, pp. 801-814

806

Figure 3. Geometric domain with pallets arranged in racks

The main dimensions of the modeled pharmaceutical storage were 47600 mm in the *x*-direction, 52040 mm in the *y*-direction, and 12791 mm in the *z*-direction. The geometric model used for all numerical simulations in this work is shown in fig. 3. Storage was filled with a total of 28 pallet racks, which can hold up to 147 pallets each. Pallets arrangement inside geometric domain can be seen in fig. 3.

Numerical model

Comprehensive CFD code ANSYS FLUENT was used for all numerical simulations reported in this paper. ANSYS FLUENT models 3-D turbulent flow field with heat transfer solving set of PDE on collocated computational finite volume grid. Modeled PDE are the RANS equations representing mass, momentum, turbulence, and energy conservation.

The heating rate of pallets was determined by convective heat transfer between fluid (air) and pallets' surfaces. A preliminary steady-state CFD simulation was conducted to determine the value of the heat transfer coefficient between fluid and pallets' surfaces. Pallets surface temperature was set to a constant value of 291.15 K and the inlet air temperature was set to 294.5 K. Heat flux on the pallets surfaces, obtained as a result of simulation, was used to determine the value of heat transfer coefficient:

$$h_{sf} = \frac{\left| q_{sf} \right|}{T - T_{ps,init}} \tag{1}$$

Unsteady simulation was initialized from converged steady-state simulation of storage space with pallets walls and air temperature of 291.15 K. Adaptive time step in range 0.0001-0.1 second was used for unsteady solution satisfy the courant-Friedrichs-Lewy condition of 1.

Turbulence modelling

The *k-ω* SST turbulence model is the model of choice for turbulence modelling inside cold rooms, clean rooms, and storage spaces as it has shown better accuracy with similar computational costs compared to other RANS turbulence models (standard *k-ε*, realizable *k-ε*, RNG *k-ε*, standard *k-ω*, and 7-equation Reynolds stress model) [3, 5, 7, 18, 19]. Based on this, *k-ω* SST turbulence model was used for turbulence modelling in this work. The main feature of the *k-ω* SST model is that it incorporates both standard *k-ε* and standard *k-ω* turbulence model properties. The *k-ω* SST model utilizes a blending function merge standard *k-ω* and transformed *k-ε* models into a single model. This allows the *k-ω* SST model to maintain robust and accurate turbulence formulation of the standard *k-ω* model in the near-wall zones and free-stream independence of *k-ε* model in far-field flow [20].
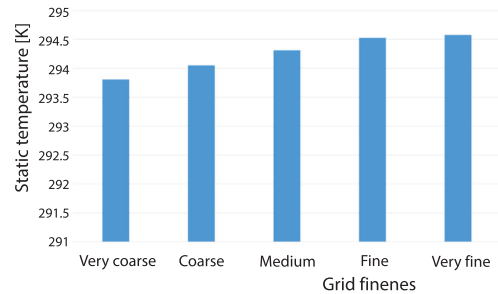
Computational grid and grid independence study

A computational grid composed of all hexagonal elements was constructed to minimize numerical diffusivity [21]. A numerical grid was generated by gradually increasing the num-

Tabašević, I. D., *et al.*: Experimental and Numerical Investigation of Thermal and ...
THERMAL SCIENCE: Year 2022, Vol. 26, No. 1B, pp. 801-814

807

ber of finite volumes until the solution stopped changing with the increase in the number of control volumes. Grid independent solution was ensured using this procedure. Steady-state simulations of storage heating were performed on five different grids: very coarse, coarse, medium, fine, and very fine, composed of 2633141, 5734744, 8473994, 11558536, and 15678383 elements, respectively. Changes in average temperature in middle $x = const.$ cross-section were monitored for grid independence study, fig. 4. Solution stopped changing more than 2% switching from fine to very fine grids. Based on this, the fine grid was adopted for all CFD simulations performed in this work. The adopted grid with detailed views is shown in fig. 5.


Figure 4. Grid independence study, static temperature *vs*. grid fineness
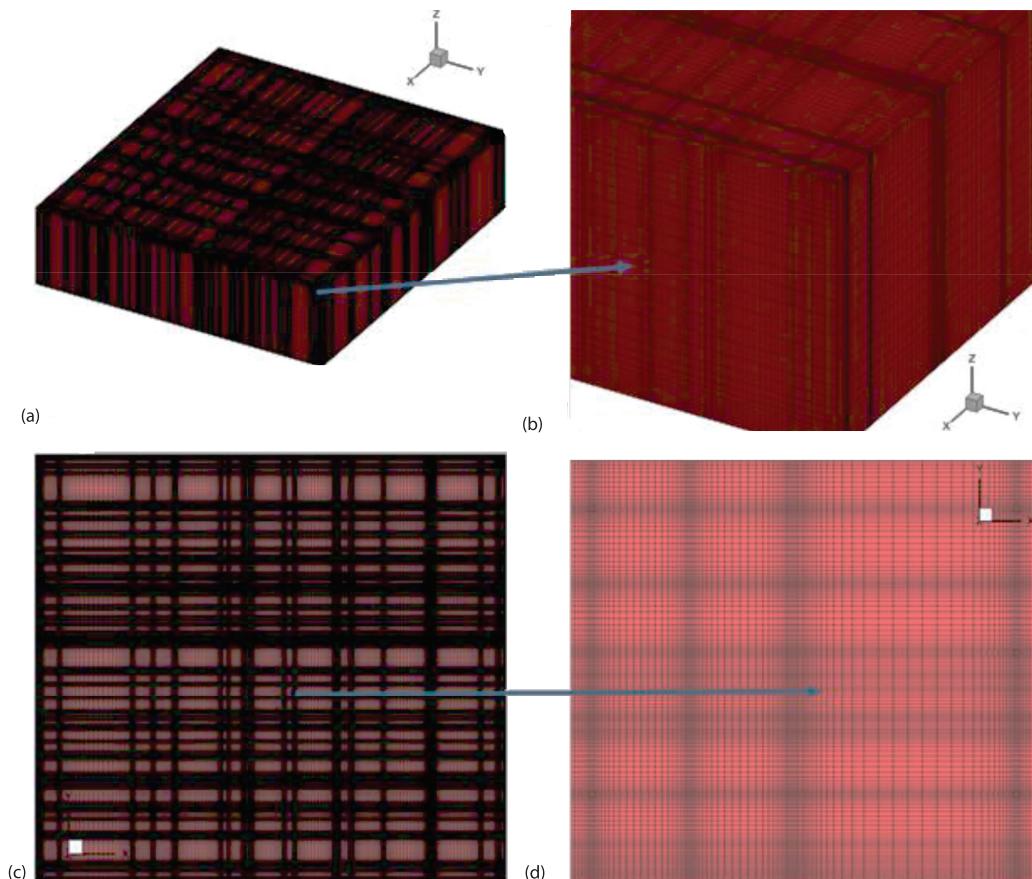
Figure 5. Computational mesh used for numerical simulations; (a) isometric view, (b) isometric view – refinement zone detail, (c) top view, and (d) top view – refinement zone detail (*for color image see journal web site*)

Boundary conditions

Computational domain with boundaries is shown in fig. 6. As can be seen, the domain has four lateral walls, one top, and one bottom wall, corresponding to the storage side walls, ceiling, and floor surfaces, in that order. Wall boundary condition was also applied to all pallets surfaces. Domain has a total of 49 circular inlets arranged in the six rows on the top of the domain. Inlets in the first and the last rows are characterized by the swirling flow pattern and all remaining inlets have only one velocity component, normal to the inlet surface (jet inlets). The total of 36 square outlets are positioned on the top domain surface, arranged in six rows. Finally, 18 square outlets are positioned at the bottom domain surface, deployed in the seven different rows.
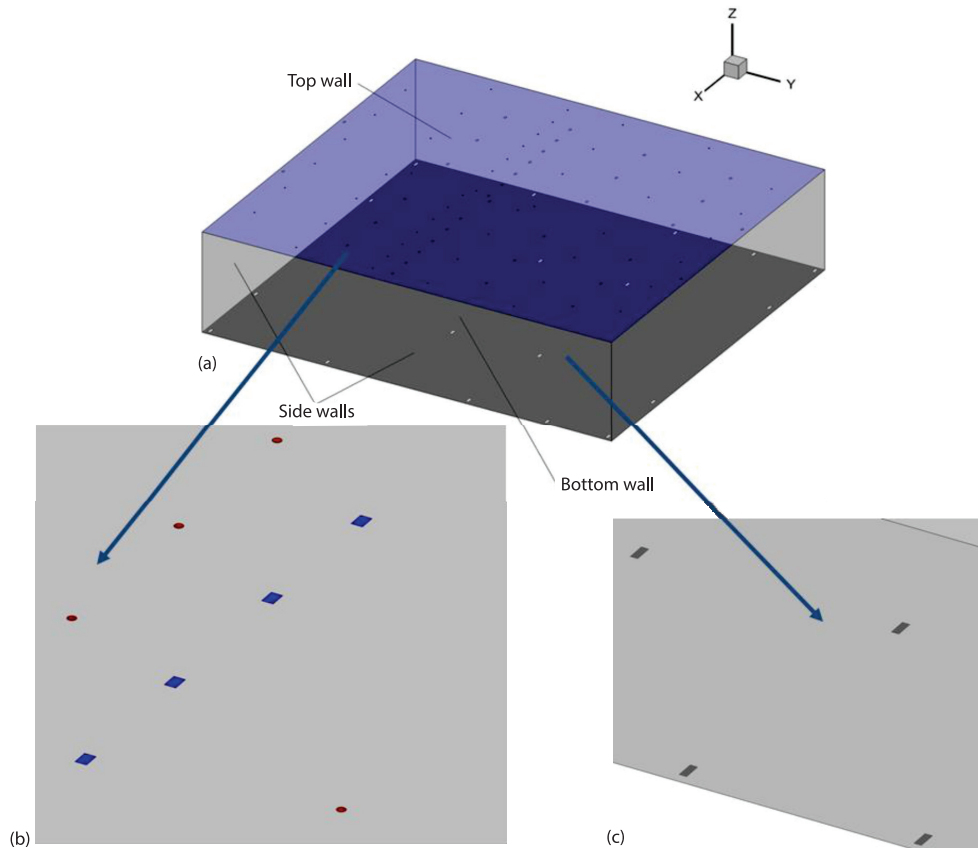
Figure 6. Domain boundaries; (a) storage walls, (b) detailed view of top storage surface, circular inlets are colored in red and square outlets are colored in blue, and (c) detailed view of the bottom surface, square outlets are colored in dark grey

Velocity magnitude was specified as a boundary condition at all inlet surfaces. Axial velocity component of 17.26 m/s and tangential velocity component of 2.93 m/s were applied for swirl inlets, while axial velocity component of 9.337 m/s was defined for all jet inlets. The temperature of 294.65 K and turbulent intensity of 10% was used for all inlets. Values for inlet velocity and temperature were taken from the experimental data, and the value for turbulent intensity was adopted from [22, 23]. Zero-gradient boundary condition was applied for

Tabašević, I. D., *et al.*: Experimental and Numerical Investigation of Thermal and ...
THERMAL SCIENCE: Year 2022, Vol. 26, No. 1B, pp. 801-814

809

all quantities at domain outlets, except for the pressure. Zero-gradient boundary condition was used for pressure at all domain inlets, and a constant value equal to atmospheric pressure of 101325 kgm/s^2 was specified at domain outlets.

Air density was allowed to change according to the ideal gas law in order to include buoyancy effects. The buoyancy force term arising from density changes was implemented into momentum equation using Boussinesq approximation, which assumes that the variation in fluid density affects only the buoyancy term and the fluid density is a function of temperature only.

Results and discussion

Two different scenarios were investigated in the scope of this work:
– the scenario of the full system recovery, in which storage pallets were heated to the design temperature of 294.65 K and
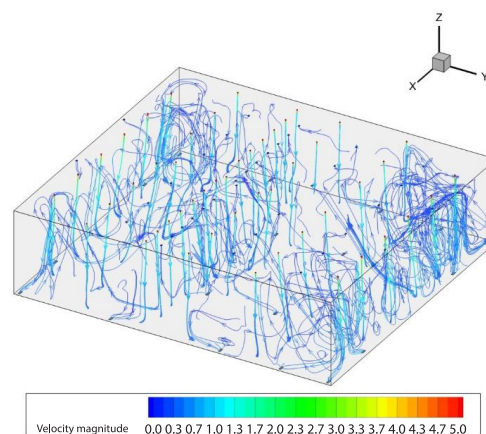– the scenario in which storage pallets were heated to the minimum required temperature of 293.15 [K], according to ASHRAE [24].

The necessary time for the full system recovery (up to the temperature of 294.65 K) is 48 hours. Unsteady CFD simulations for such long periods are still undoable due to computational hardware limitations [25], hence, full system recovery (Scenario 1) was calculated using steady-state approximation. Since the storage system reaches the necessary minimum temperature in about three hours, the second scenario was calculated in an unsteady manner.

Full system recovery

As previously stated, the first case considers the full system recovery. This means that, after system failure, pallets' temperature dropped to 291.15 K. System recovery started from this temperature and lasted for 48 hours until design temperature of 294.65 K was reached – full system recovery. Due to long recovery time (48 hours), unsteady CFD simulations were undoable. Thus, it was decided to calculate final velocity patterns and temperature distribution using steady-state approach.

The calculated flow field streamlines are shown in fig. 7. It can be seen that the obtained flow field is highly non-uniform, characterized by large vortex structures. Such flow field velocity distribution is mainly caused by the small number of outlets (compared with the number of inlets) and their distribution. Namely, outlets are positioned both on the top and the bottom surfaces of the storage, as already explained. Since the air-flow directly influences the convective heat transfer inside the storage space, it is expected that the uneven velocity distribution will consequently cause inhomogeneous heating and differences in pallets surface temperature.


Figure 7. Velocity streamlines colored by velocity magnitude inside the storage domain

Temperature distribution in the middle x = constant and four selected y = constant cross--sections are presented in fig. 8(a)-8(d). As expected, based on the previous discussion, the air temperature inside storage is non-uniform with values in the range between 293.67 K and 294.65 K. Higher temperature values are present near velocity inlets and near storage walls. Velocity vectors, colored by temperature for
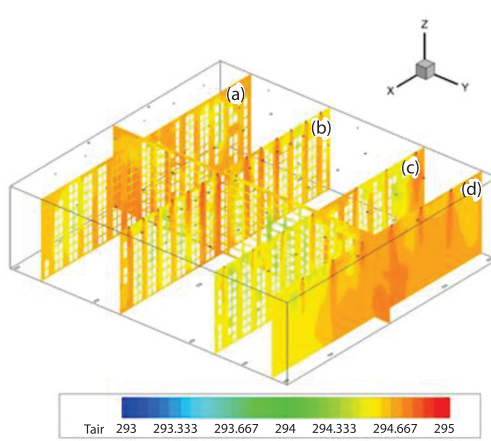
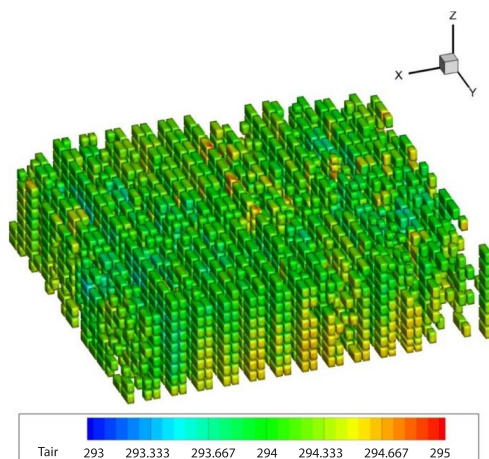**Figure 8. Static temperature distribution inside storage**

middle x = constant and middle y = constant cross-sections are shown in fig. 9. Four large closed swirl zones are formed near storage walls. These dead zones are generated because there are only two air outlets in these regions. Thus, large mass-flow injected from the storage inlets in this section has a long residence time before it is sucked out from the system. Higher temperature values are found in the upper parts of the storage and lower temperature values are present closer to the storage bottom surface. This influences convective heat transfer, which is more intensive in the upper parts of storage space. It should be noted that these are general remarks, which may not be applicable for all storage sections, due to the high non-uniformity of velocity field and temperature distribution.
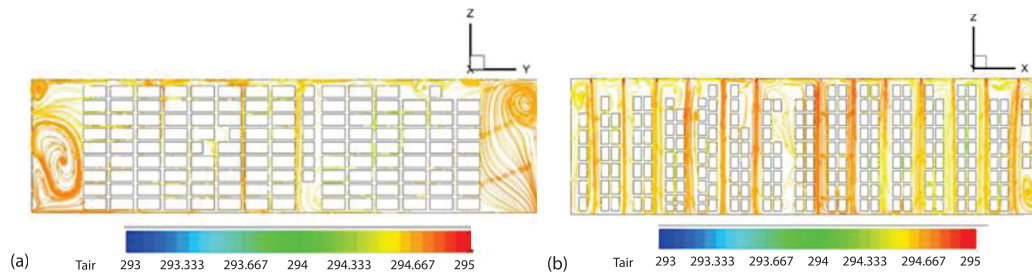
Figure 9. Velocity vectors colored by static temperature; (a) middle x = constant plane and (b) middle y = constant plane

Figure 10. Pallets surface temperature contours, steady-state simulation

Pallets' surface temperature contours are presented in fig. 10. It can be seen that, as already stated, non-uniform fluid-flow and air temperature distribution cause differences in pallets' heating rate and their final temperature. The temperature range of pallets' surfaces is between 293.5 K and 294.65 K. Higher temperature values are found in zones with high air velocity magnitude and high air temperature. This is explained by the fact that convective heat transfer coefficient increases with flow Reynolds number [26] and with the temperature difference between air and corresponding surface, eq. (1). It is also worth mentioning that pallets' surfaces near storage walls have higher temperatures due to high-temperature closed air vortices formed in near-wall storage zones, figs. 9. and 10.
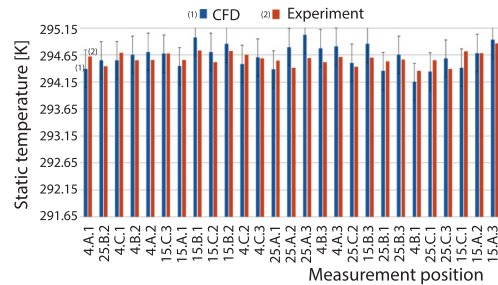
Comparison between experimentally measured and numerically calculated pallets surface temperature is shown in fig. 11. The maximum relative difference is less than 5%, which means that the suggested model can be used as a quantitative predictionol for storage design.

Figure 11. Comparison of experimentally measured and numerically simulated pallets surface temperature

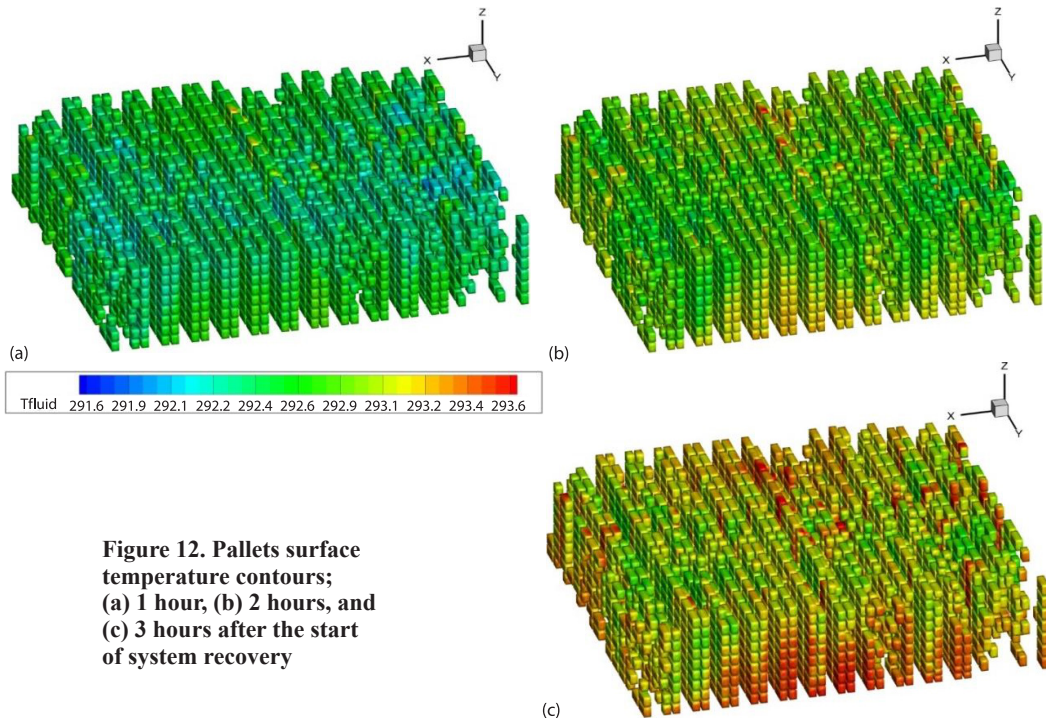### *System recovery to a minimum defined temperature*

Similarly to the previous scenario, the second case considers that, after system failure, pallets' temperature dropped to 291.15 K. Unlike previous case, this scenario considers system recovery to the minimum allowed pallets temperature of 293.15 K.

System recovery to the minimum allowed pallets temperature of 293.15 K was simulated in the next phase of this work. Relatively quick storage temperature recovery time of about 3 hours allowed for the performance of the unsteady (time dependent) simulations.
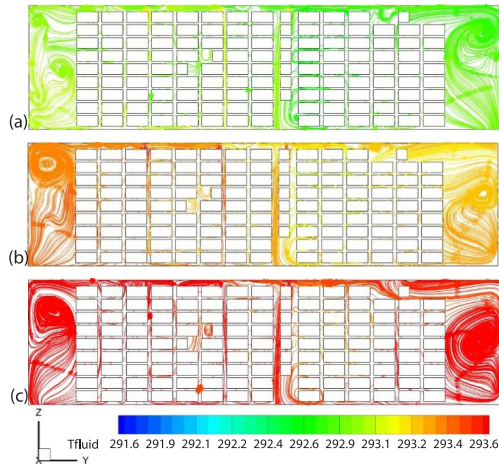
Change in pallets' surface temperature after 1 hour, 2 hours, and 3 hours is shown in fig. 12. It can be seen that pallets' temperature increases with time and that after three hours all pallets have a temperature higher than the minimum allowed of 293.15 K. Pallets' surface temperature is non-uniform, similarly to the previous scenario (steady-state simulation). However, although this uneven temperature distribution is not desirable, it is important to once more point out that high inlet mass-flow enables for all pallets to be heated above the minimum allowed temperature.
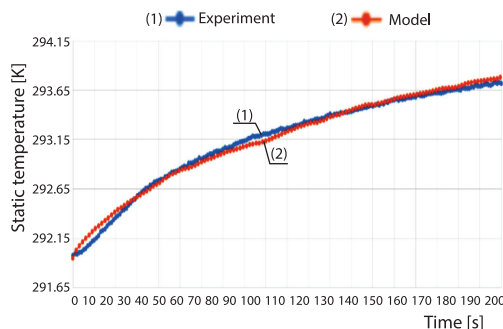

Figure 12. Pallets surface temperature contours; (a) 1 hour, (b) 2 hours, and (c) 3 hours after the start of system recovery

812

Tabašević, I. D., *et al.*: Experimental and Numerical Investigation of Thermal and ...
THERMAL SCIENCE: Year 2022, Vol. 26, No. 1B, pp. 801-814

Figure 13. Velocity vectors colored by static temperature, middle *x* = constant cross-section; (a) 1 hour, (b) 2 hours, and (c) 3 hours after the start of system recovery

Figure 14. Averaged pallets surface temperature in middle cross-section *x* = *constant vs.* time dependence, comparison between experimental and model results

Velocity vectors colored by the temperature values for middle cross-section x = constant show air heating inside the storage for periods of 1 hour, 2 hours, and 3 hours after the start of system recovery, fig. 13. It can be seen that, due to the constant supply of fresh hot air into storage, air temperature steadily increases. Air temperature in the middle cross-section, unlike surface temperature, is almost constant. This further highlights the importance of flow field uniformity during convective heating of storage products.

Comparison between experimental and numerical values of averaged pallets surface temperature in middle cross-section x = constant is shown in fig. 14. It can be seen that experimental and model curves are in close agreement, with a maximal relative difference of less than 4%, which is good enough for quantitative predictions.

Discussion

Although the developed CFD model showed good agreement with the measured data, it has some limitations, which should be commented on.

Namely, modeled geometry was simplified compared to real storage, by omitting roof zone. This simplification does not affect significantly the final solution since the air in this zone is stagnant and does not have a prominent role in the pallets' heating process. However, a more rigorous approach would be to model a realistic near-roof zone since it would allow for the placement of the top wall boundary condition at the position of the real storage roof surfaces.

The generated computational mesh consists of a large number of control volumes and requires high computational resources and long computational time to obtain the unsteady simulation solution. Because of this, the first scenario – full storage recovery, was calculated using steady-state approach. This limits the obtained CFD results to final values at time corresponding to the end of system recovery. Although calculated values agree well with the experimental data, it would be beneficial to the reader to have time dependent simulation results of the whole storage heating process.

Finally, turbulence was modeled using two-equation eddy viscosity k-ω SST turbulence model, which is the model of choice for large closed spaces. However, this model is limited by the assumption that turbulence is isotropic (Boussinesq approximation).

Future work is planned to address the limitations:
– With the advancement of the available hardware resources, storage space geometry will be modeled as close as possible to the real storage.

− Time dependent (unsteady) simulations will be performed for all scenarios.
− More advanced turbulence model, scale adaptive simulation variant of the *k-ω* SST model, will be utilized for turbulence modelling, offering a more in-depth insight into vortex structure inside the pharmaceutical storage.

Conclusions

The CFD-based simulations of the pharmaceutical storage heating were performed to determine its ability to recover to designed temperature levels. Steady-state simulations showed that the system can achieve the defined design temperature. However, it was found that storage pallets' surface temperature differs depending on pallets' position inside the storage. These differences are the consequence of a non-uniform flow field and air temperature distribution inside the storage.

Model accuracy was established by comparison with the experimental data. The maximum relative difference was smaller than 5%, meaning that the proposed model can be used as a predictive tool for pharmaceutical storage design.

Unsteady CFD simulations were performed for the case of the storage temperature recovery up to the minimum allowed temperature. The minimum allowed temperature was reached in less than three hours, although pallets' surface temperature was non-uniform, similarly to the case of steady-state simulation.

The CFD results pointed out that velocity decreases fast after inlet decreasing pallets convective heating potential. However, inlet mass-flow is large enough to introduce a necessary amount of fresh air to keep pallets' temperature at desired levels.

The CFD simulations also showed the existence of closed swirl zones near-wall surfaces. These empty zones could be filled with additional pallet racks to increase storage capacity. A requirement is to open more air outlets in these zones, which would enhance flow intensity and heat convection.

It is planned to implement the scale adaptive simulation variant of the *k-ω* SST model, which would enable in-depth analysis of flow field swirl structures. The developed model will be used for design of new and reconstruction of existing pharmaceutical storages. The suggested model will be used for calculation of conditions inside pharmaceutical clean rooms in future works.

Acknowledgment

Nomenclature

h　 − heat transfer coefficient, $[\mathrm{Wm^{-2}K^{-1}}]$
q　 − heat flux, $[\mathrm{Wm^{-2}}]$
T　 − temperature, $[\mathrm{K}]$

Subscripts

init − initial value
f　 − fluid
p　 − pallet
s　 − surface

References

[1] Baruffaldi, G., *et al.*, The Storage of Perishable Products: A Decision-Support Tool to Manage Temperature-Sensitive Products Warehouses, Sustainable Food Supply Chains: *Planning, Design, and Control through Interdisciplinary Methodologies*, *1* (2019), 1, pp. 131-143
[2] Shen, T., *et al.*, Recent Application of Computational Fluid Dynamics (CFD) in Process Safety and Loss Prevention: A Review, *Journal of Loss Prevention in the Process Industries*, *67* (2020), 104252
[3] Ho, S. H., *et al.*, Numerical Simulation of Temperature and Velocity in a Refrigerated Warehouse, *International Journal of Refrigeration*, *33* (2010), 5, pp. 1015-1025

[4] Wu, X., *et al.*, The Numerical Investigation of Temperature and Velocity Distribution in the High-Bay Depot, *Advances in Mechanical Engineering*, *6* (2014), 1, 541726

[5] Hoang, H. M., *et al.*, Preliminary Study of Air-Flow and Heat Transfer in a Cold Room Filled with Apple Pallets: Comparison between Two Modelling Approaches and Experimental Results, *Applied Thermal Engineering*, *76* (2015), Feb., pp. 367-381

[6] Kaood, A., *et al.*, Numerical Investigation of the Flow Fields and Thermal Patterns in a Large Cold Store (I), *Proceedings*, ASME Power Conference, Charlotte, N. C., USA, 2016, 50213

[7] Parpas, D., *et al.*, Experimental Investigation and Modelling of Thermal Environment Control of Air Distribution Systems for Chilled Food Manufacturing Facilities, *Applied Thermal Engineering*, *127* (2017), Dec., pp. 1326-1339

[8] Sularno, A., *et al.*, Experimental and Numerical Investigation of Cooling Performance of a Cold Storage in a Pharmaceutical Industry, *Journal of Physics: Conference Series*, *1090* (2018), 12012

[9] Parpas, D., *et al.*, Investigation into Air Distribution Systems and Thermal Environment Control in Chilled Food Processing Facilities, *International Journal of Refrigeration*, *87* (2018), Mar., pp. 47-64

[10] Ghiloufi, Z., Khir, T., The CFD Modelling and Optimization of Pre-Cooling Conditions in a Cold Room Located in the South of Tunisia and Filled with Dates, *Journal of Food Science and Technology*, *56* (2019), 8, pp. 3668-3676

[11] Tanaka, F., *et al.*, The use of CFD to Improve the Performance of a Partially Loaded Cold Store, *Journal of Food Process Engineering*, *35* (2012), 6, pp. 874-880

[12] Špiljar, Ž., *et al.*, Analysis of Jet Fan Ventilation System Installed in an Underground Car Park with Partition Walls, *Journal of Sustainable Development of Energy, Water and Environment Systems*, *6* (2018), 2, pp. 228-239

[13] Guo, J., *et al.*, Characteristic Analysis of Humidity Control in a Fresh-Keeping Container Using CFD Model, *Computers and Electronics in Agriculture*, *179* (2020), 105816

[14] Sajadiye, S., Zolfaghari, M., Simulation of in-Line *vs*. Staggered Arrays of Vented Pallet Boxes for Assessing Cooling Performance of Orange in Cool Storage, *Applied Thermal Engineering*, *115* (2017), Mar., pp. 337-349

[15] ***, Health Products Regulatory Authority, Guide to Good Distribution Practice of Medicinal Products for Human Use Guidelines for good practice in distribution, Official Gazette of the Republic of Serbia, pp. 30/10, 107/12, 2016

[16] ***, ISO IEC., General Requirements for the Competence of Testing and Calibration Laboratories, International Organization for Standardization, Geneva 27, Switzerland, 2017

[17] ***, WHO Technical Report Series No. 961, Annex 9: Model Guidance for the Storage and Transport of Time and Temperature-Sensitive Pharmaceutical Products – Qualification of Temperature-Controlled Storage Areas, World Health Organization, Geneva 27, Switzerland, 2011

[18] Delele, M. A., *et al.*, Optimization of the Humidification of Cold Stores by Pressurized Water Atomizers Based on a Multiscale CFD Model, *Journal of Food Engineering*, *91* (2009), 2, pp. 228-239

[19] Delele, M. A., *et al.*, Studying Air-Flow and Heat Transfer Characteristics of a Horticultural Produce Packaging System Using a 3-D CFD Model – Part I: Model Development and Validation, *Postharvest Biology and Technology*, *86* (2013), Dec., pp. 536-545

[20] Menter, F. R., Two-Equation Eddy-Viscosity Turbulence Models for Engineering Applications, *AIAA Journal*, *32* (1994), 8, pp. 1598-1605

[21] Sadrehaghighi, I., Structure Meshing for CFD, Report No. 2.20, Annapolis, USA, 2020

[22] Foster, A. M., *et al.*, The 3-D Effects of an Air Curtain Used to Restrict Cold Room Infiltration, *Applied Mathematical Modelling*, *31* (2007), 6, pp. 1109-1123

[23] Jiying, L., *et al.*, A Review of CFD Analysis Methods for Personalized Ventilation (PV) in Indoor Built Environments, *Sustainability*, *11* (2019), 15, 4166

[24] ***, ASHRAE, HVAC Applications, The American Society of Heating, Refrigerating and Air-Conditioning Engineers, Atlanta, USA, 2019

[25] Getahun, E., *et al.*, Importance of Integrated CFD and Product Quality Modelling of Solar Dryers for Fruits and Vegetables: A Review, *Solar Energy*, *220* (2021), May, pp 88-110

[26] Wakao N., Kaguei, S., *Heat and Mass Transfer in Packed Beds*, John Wiley and Sons., New York, USA, 1983